

# BEAM HALO MEASUREMENTS USING ADAPTIVE MASKING METHODS AND PROPOSED HALO EXPERIMENT

H. Zhang, B. Beaudoin, S. Bernal, R. Fiorito, R. Kishek, K. Poor Rezaei, A. Shkvarunets  
University of Maryland, College Park, MD 20742, USA

## Abstract

Beam halo is a common phenomenon in particle beams, especially for modern, advanced accelerators where high beam intensities lead to strong space charge. Halo is generally understood as a population of particles that do, or will, reach large transverse radii relative to a more intense, centralized beam core. It is associated with emittance growth, beam quality degradation and particle loss. The particle-core model is commonly used to describe halo formation as the result of a parametric resonance due to envelope mismatch. Few experiments have been carried out to test this theory. Measurement of beam halo is particularly problematic for faint halos, where light from the intense core obscures the optical image of the halo. In this paper, we review a diagnostic for high-dynamic range halo measurements based on adaptive masking of the beam core. We present the design of an experiment to study halo formation from envelope mismatch for beams spanning a wide range of intensities on the University of Maryland Electron Ring (UMER).

## INTRODUCTION

Modern intense-beam accelerators, where space charge is important, have a wide variety of applications such as spallation neutron sources, rare isotope accelerators, and intense proton drivers for muon and neutrino physics. A prevalent space charge induced problem is beam halo formation. Halo is generally understood as a population of particles that do, or will, reach large transverse radii relative to a more intense, centralized beam core. It is associated with emittance growth, beam quality degradation and particle loss [1]. Since the density of the halo is often faint compared to the core, it makes particle-in-cell simulation, as well as experimental detection, difficult. Several analytic models such as particle-core model [2] and free energy model [3] are derived either to depict the process of halo formation or to describe the associated emittance growth. Many theory and simulation studies developed these ideas and discussed various mechanisms for halo formation. However, fewer experimental studies have been performed. For example, the LEDA experiment [4] demonstrated agreement with the particle-core model. But unfortunately its propagation length is limited and it is no longer operational. In this paper, we will review a halo diagnostic method with high dynamic range using adaptive mask. Then, we propose a new experiment for testing halo theories.

## BEAM HALO MEASUREMENTS USING ADAPTIVE MASKING METHODS

Comparing with the beam core, the intensity of beam halo is very faint. It can be as low as  $10^{-5}$ ~ $10^{-6}$ , which is very difficult to detect by normal diagnostic methods because of its low dynamic range. Borrowed from astronomy's idea of coronagraphy, we develop this imaging method using a device called digital micromirror-array device (DMD). It successfully masks out the core adaptively and reconstructs the transverse beam distribution with high dynamic range as  $10^6$ .

We first show the simplified optical design in Fig. 1. In this configuration, we first focus the original beam source onto the DMD surface. The source can be any light source such as fluorescent screen or initiative light sources like OTR and SR. DMD is a commercialized device manufactured by Texas Instrument and widely used in projector and TV industry. It contains  $1024 \times 768$  tiny mirror, and each mirror can be independent addressable and tilted to two angles. This feature allowed us to use it as spatial filter to redirect the halo image onto the camera while block out the brighter light of beam core (as indicated in the figure with different colors). We applied several compensations to avoid or minimize the effect caused by DMD, such as tilting DMD 45 degree around the optical axis, rotate camera by a scheinpflug angle. The details can be seen in reference [5].

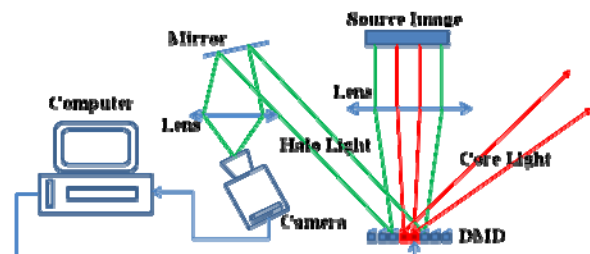


Figure 1: Diagram of adaptive masking method[5].

We have been applied this method at UMER [5], JLab FEL [6] and SPEAR3 [7]. In UMER, we first tested this method using images generated by intercepting the 6 mA, 100 ns, 10 keV beam onto a phosphor screen in UMER. We showed a series of images with different quadrupole strength in the upstream in Fig. 2. The upper halves indicated the beam cores, while the lower ones only displayed the distributions outside with a mask blocking out the beam core. This was the first experimental result to separate the core and halo distributions adaptively, and measure them with normal dynamic range. The combine dynamic range can be as high as  $10^5$ .

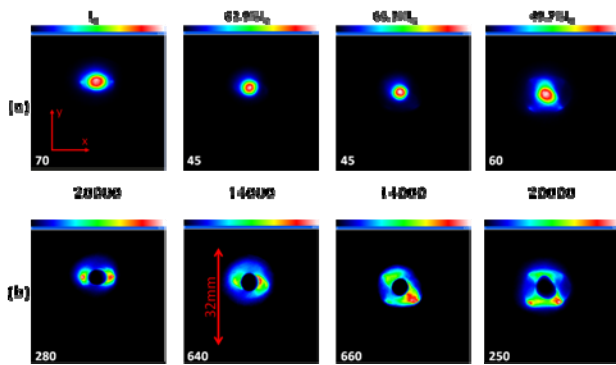


Figure 2: Beam (a) and halo (b) images with quadrupole current variation[5].

We applied a similar experimental setup in JLab FEL, using their synchrotron radiation as source image. Several consequent masks are applied to the DMD when taking beam images, in order to access the limitation of dynamic range for this method. Figure 3 shows diagonal line scans of beam images with increasing size of masks in logarithmic scale. The original images are taken with an increasing shutter time, while the scans are normalized by the shutter time and subtracted with the background. The tail of the scan indicates we achieved a dynamic range higher than  $10^6$ .

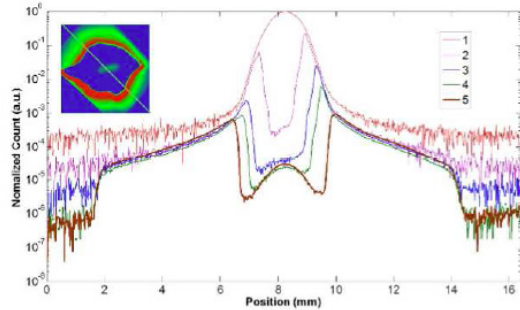


Figure 3: Dynamic range scan with consequence of increasing mask size[6].

In the SPEAR3 ring at SLAC, we used this method to study the injection. Due to the high contrast of the synchrotron radiation between stored beam and injected beam, the ratio of which was usually higher than  $10^4$ , we wanted to use the DMD to block the intense stored beam and study the injected beam dynamic. The advantage of using this adaptive masking method is to make the online measurement possible without affecting any other user in the SPEAR3. Figure 4 is reconstructed pseudo-color

picture of the stored beam in logarithmic scale, indicating a PSF of this optical system. The cross implied a diffraction pattern of the first limitation aperture shown in upper right corner. Moreover, a high dynamic range of  $10^6$  was achieved again from this measurement.

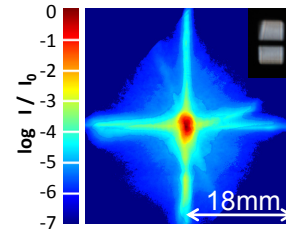


Figure 4: Reconstruct high dynamic range picture of SPEAR3 stored beam[7].

Figure 5 shows the damping process of the injected beam for the synchrotron port right after Booster-to-Storage ring (BTS) transportation at SPEAR3 with the stored beam masked by the DMD, for different Quadrupole settings in Booster-to-Storage ring (BTS) transport beam line. The detailed analysis is presented in reference [7]. It shows the utility of this method for studying the injection effectiveness, matching and different injection mode such as alpha mode.

### A NEW EXPERIMENT IN UMER PROPOSED FOR TESTING HALO FORMATION THEORIES

In this section, we proposed an experiment to systematically study beam halo formation in UMER. UMER is a unique machine, designed for exploring the physics of beams with intense space charge using low-energy, high-current electron beams [8]. It consists of a 10 keV electron gun, a short injection and matching section, and a 1.83 m-radius ring. Since UMER was developed as a research machine for beam physics, it was designed to be flexible. For example the bunch length can be adjusted over a wide range (25-125 ns). By generating beams using photo-emission, we can produce 5-ns pulses, or apply short longitudinal perturbations to a long-pulse beam. We can also adjust the beam current using an aperture wheel inside the gun, hence allowing us to vary the space charge intensity over a wide range (0.5 – 100 mA). The scalability of the space charge dynamics allows us to extrapolate results from UMER to many other types of machines such as proton linacs or FEL

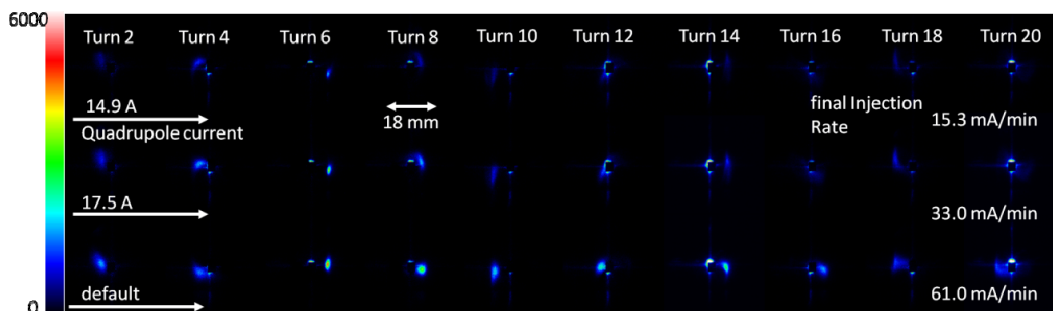


Figure 5: Images of the beam in the SPEAR3 during the first 20 turns for three matching conditions[7].

injectors.

For study different source for halo formation, the key challenge is to control the beam from the source and let it go through the injection line into the ring with minimum halo. From then on, it is straightforward to introduce the sources for halo formation and observe the consequences. The meaning of minimizing the halo in the beginning of the ring is to investigate the halo source independently such as machine errors, rms mismatch, skew beam rotation, sextupole and higher-order errors, etc. Here we will start the discussion with the empirical method to match the beam from the injection to ring.

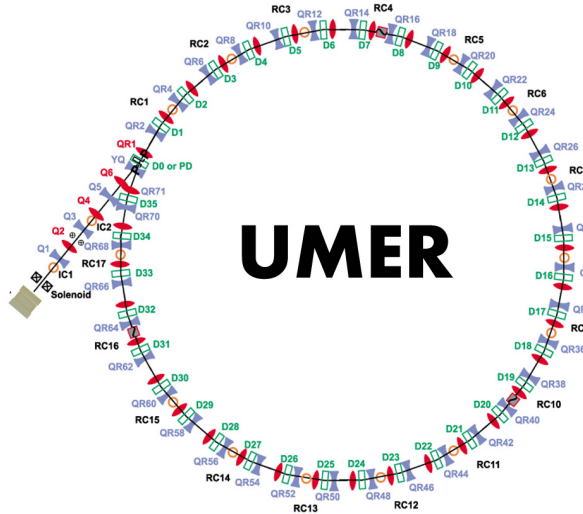


Figure 6: Schetch of UMER magnet and configuration

Starting from the calculated value for quadrupoles in the injection and ring to match the beam, we first assume a small mismatch (linear approximation) due to magnet error and misalignment, and then we apply a matrix implementation. In the injection, we use the quadrupoles Q2 – Q5 for online adjustment and the matrix form is as follows:

$$\begin{pmatrix} X_i \\ Y_i \end{pmatrix}_{I_2, I_3, I_4, I_5} = \begin{pmatrix} X_m \\ Y_m \end{pmatrix} + \begin{pmatrix} R_{x12} & R_{x13} & R_{x14} & R_{x15} \\ R_{y12} & R_{y13} & R_{y14} & R_{y15} \end{pmatrix} \begin{pmatrix} \Delta I_2 \\ \Delta I_3 \\ \Delta I_4 \\ \Delta I_5 \end{pmatrix} \quad (1)$$

Where  $X_i$  and  $Y_i$  are the  $2 \times$  rms transverse beam sizes in the  $i$ 's screen, which is measured with magnet strength setting of  $I_2, I_3, I_4, I_5$ .  $X_m$  and  $Y_m$  is the matched beam size on each screen.  $\Delta I$  is the magnet strength change from original setting to a updated setting to minimize the mismatch.  $R_{wij}$  is the beam size response in  $i$ 's screen when changing quadrupole  $j$  ( $w$  can be  $x$  or  $y$ ), defined as

$$R_{w,j} = \frac{\partial W_i}{\partial I_j} \quad (2)$$

and can be measured by perturbing the current quadrupole strength and observing the beam size in each screen. The full matrix form can be rewritten and extended as

$$\begin{pmatrix} X_1 \\ Y_1 \\ X_2 \\ Y_2 \\ \dots \\ X_n \\ Y_n \end{pmatrix} = \begin{pmatrix} R_{x11} & R_{x12} & R_{x13} & R_{x14} & 1 & 0 \\ R_{y11} & R_{y12} & R_{y13} & R_{y14} & 0 & 1 \\ R_{x21} & R_{x22} & R_{x23} & R_{x24} & 1 & 0 \\ R_{y21} & R_{y22} & R_{y23} & R_{y24} & 0 & 1 \\ \dots & \dots & \dots & \dots & \dots & \dots \\ R_{xn1} & R_{xn2} & R_{xn3} & R_{xn4} & 1 & 0 \\ R_{yn1} & R_{yn2} & R_{yn3} & R_{yn4} & 0 & 1 \end{pmatrix} \begin{pmatrix} \Delta I_1 \\ \Delta I_2 \\ \Delta I_3 \\ \Delta I_4 \\ X_m \\ Y_m \end{pmatrix} \quad (3)$$

E R Δ

This is standard linear equations, and the optimal solution can be obtained in a least square sense, i.e.  $\Delta = (R^T R)^{-1} R^T E$ . A updated injection setting is given by  $I_1 - \Delta I_1, I_2 - \Delta I_2, I_3 - \Delta I_3, I_4 - \Delta I_4$ . Details for this method can be referred to [9].

We test this method with the simulations in Warp [10] by scanning the quadrupoles Q2-Q5, and monitoring the envelope change in periodic point, e.g. the screen position in the ring (located in ring chamber (RC\*) in Fig. 6). Fig. 7 shows the comparison before (red star points) and after the empirical correction (blue circle point). There is an obvious improvement since the deviation of the beam sizes is much smaller after the empirical correction both in X and Y directions. In real experiment, we might need several implementations of this method to let the solution converge.

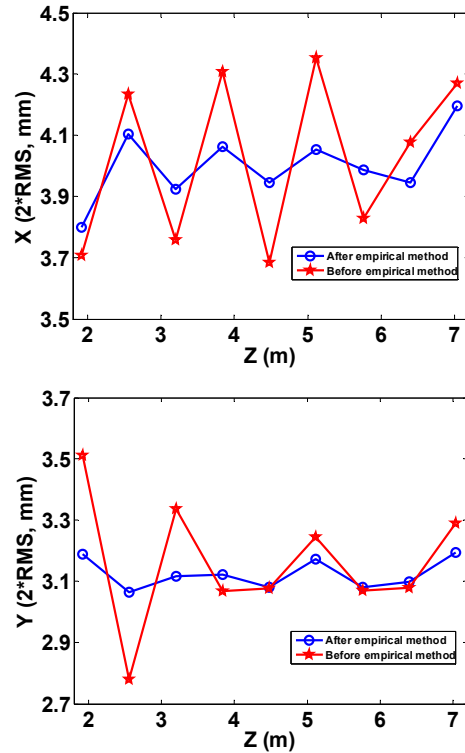


Figure 7: Beam sizes in screen before and after empirical method.

Once we reach a matching condition, we can control the mismatch factor by changing the quadrupoles'

strength in the injection or the FODO lattice (mainly quadrupole strength) in the ring. The mismatch factor is a parameter quantifying the error of the injected beam in size or divergence relative to the matched values in the ring. In theory, there are two eigen functions of the mismatch modes: the breathing mode, in which the oscillations for the horizontal and vertical envelopes are in phase, and the quadrupole mode in which the envelopes for horizontal and vertical are  $180^\circ$  out of phase. The former describes the envelope oscillation with a radial symmetry. In general, a mismatch consists of a linear combination of the two modes. .

The experimental procedure is to calculate the matching conditions, and then systematically change the injection quadrupoles in order to produce a controlled mismatch. For each setting, I will measure the beam halo at the available screens. In the first turn, interceptive imaging diagnostics, in combination with tomography [11] will provide phase space maps and emittance measurements. Beyond the first turns, knockout measurements [12] will provide beam images. In an upgrade scheduled for Sep. 2012, we are installing three additional knockout statements so we will have four images per turn over multiple turns. If necessary, the adaptive masking method described above will be applied to detect faint halos. Along with these measurements, we will also monitor turn-by-turn beam losses using a wall-current monitor.

Another possible parameter we can control is the skew error generated by mis-rotation of the quadrupoles. Previous study proved the sensitivity of halos to this factor [13]. Given the fact that UMER uses thin, air-core and printed-circuit magnets; it is easy to develop a skew corrector by overlaying a pair of quadrupoles at a  $45^\circ$  angle inside the same mount. The angle of the magnetic field can then be varied by controlling the current to each printed-circuit. Earlier, a prototype of this idea has been tested [10], and currently we have one such skew corrector installed. The skew effect on halo formation can be addressed in such experiment.

For all the experiments, we will compare results with predictions from the particle core model and the free energy model, as well as Warp simulation.

### CONCLUSION

In this paper, we reviewed a diagnostic used for halo measurement, based on using a digital micro-mirror array for adaptive masking of light from the beam core. A high dynamic range of  $10^6$  was demonstrated in experiments at UMER, the JLab FEL, and the SLAC SPEAR3 injector. This diagnostic is not only applicable to electron beams, but also the ion beam, as long as we have a scintillator transform the beam into a 2D light source with high dynamic range. We also propose a new design of experiment for halo formation. We tested the empirical method for beam matching in simulation. In the near future, the work will focus on the experiment verification of this method and continue to study the mechanism of halo formation.

### REFERENCES

- [1] A.V. Fedotov, et al., *Proc. European Part. Acc. Conf.*, Vienna, p. 1289 (2000).
- [2] R. Gluckstern, *Phys. Rev. Lett.*, 73 (1994).
- [3] M. Reiser, *Journal of Applied Physics*, 70 (1991).
- [4] C. K. Allen, et al., *Phys. Rev. Lett.* 89, 214802 (2002).
- [5] H. Zhang, et al., *Phys. Rev. ST Accel. Beams* 15, 072803 (2012).
- [6] R. B. Fiorito, et al., *Proc. of BIW12*, Newport News, VA, TUPG031(2012).
- [7] H. Zhang, et.al. *Proc. of IPAC12*, New Orleans, LA, WEOAA01,(2012).
- [8] R. A. Kishek, et al., *Proc. of Part. Acc. Conf.*, Albuquerque, New Mexico, p.820(2007).
- [9] H. Li, Control and Transport of Intense Electron Beams, *Ph.D. Dissertation*, Univ. of Maryland, 2004.
- [10] D.P. Grote, et al., *Nucl. Instr. and Meth. A*, vol. 415, p. 428 (1998)
- [11] D. Stratakis, et.al. *Physics of Plasmas*, vol. 17, pp. 056701 (2010).
- [12] T. W. Koeth, et al. *Proc. Part. ACC. Conf.*, New York, NY, USA, 2011.
- [13] R. A. Kishek, et al. *AIP Conf. Proc.*, vol. 693, pp. 89–92 (2003).